JOURNAL OF MATERIALS SCIENCE 26 (1991) 4657–4662

Grain growth behaviour of the Al–Cu eutectic alloy during superplastic deformation

B. P. KASHYAP
Department of Metallurgical Engineering, Indian Institute of Technology, Bombay, 400 076, India

Grain growth behaviour of the Al–Cu eutectic alloy was investigated as a function of strain (ε), strain rate ($\dot{\varepsilon}$) and deformation temperature (T) over $\dot{\varepsilon} = 10^{-5}$ to $10^{-2}\,s^{-1}$ and $T = 400$ to 540 °C. The grain size increases with increase in strain and temperature. Upon deformation to a fixed strain, the grain growth is generally seen to be more at lower strain rates. The rates of overall grain growth ($\dot{d}_{\varepsilon,t}$) and due to deformation alone ($\dot{d}_{\varepsilon}$), however, increase with increasing strain rate according to $\dot{d}_{\varepsilon,t} \propto \dot{\varepsilon}^{0.86}$ and $\dot{d}_{\varepsilon} \propto \dot{\varepsilon}^{0.64}$, respectively. The increase in the grain growth rate with strain rate is attributed primarily to the shorter time involved at higher strain rate for reaching a fixed strain. The activation energy for grain growth under superplastic conditions is estimated to be 79 kJ mol^{-1}.

1. Introduction

Plastic strain of several hundred per cent, typical of superplasticity, is obtained under suitable test conditions in materials having fine ($\leqslant 10\,\mu m$) equiaxed grains. The required fine grain sizes are attained in the presence of second-phase or intermetallic compounds that restrict grain boundary migration. However, the time and stress involved in deformation at elevated temperature impart grain growth to a significant extent in several superplastic materials (e.g. [1–8]). It has been reported [4] that the grain size in a microduplex Al–Cu eutectic alloy increases from 1.5 to 6.0 μm in the course of superplastic deformation at 470 °C. Such concurrent grain growth affects the deformation behaviour at low strain rates to the extent that the sigmoidal nature of the log stress (σ) versus log strain rate ($\dot{\varepsilon}$) curve at low strain rates is sometimes attributed to this change in the microstructure [4]. Watts and Stowell [2] have shown that the strain hardening during superplastic deformation of the Al–Cu eutectic alloy can be accounted for by the observed grain growth. While the deformation behaviour of the Al–Cu eutectic alloy has been extensively studied [2, 4, 9–14], the concurrent grain growth aspect has been studied only in the case of initially elongated grains [2]. The elongated grains generally undergo not only grain growth but a reduction in the grain aspect ratio also [5] which makes the analysis of grain growth difficult. It would, however, be interesting to know how, as a result of superplastic deformation, the grain growth occurs in the Al–Cu eutectic alloy having equiaxed microstructure. With this aim, a study on the grain growth behaviour of the Al–Cu eutectic alloy is presented here.

2. Experimental procedure

An Al–Cu eutectic alloy of the nominal composition was produced in the form of 1.95 mm thick sheet as described elsewhere [12]. The microstructure in as-worked condition was equiaxed. Tensile specimens of 25 mm gauge length and 6.4 mm gauge width were machined from this sheet. The tensile specimens were deformed under selected strain-rate and temperature conditions using an Instron Universal Testing Machine, modified [15] to run at constant strain rates. The grain size (mean intercept length) of the specimens after heating to and stabilizing at the test temperatures for 45 min was 6.5 μm. This has been treated as the initial grain size (d_0) in this study. Temperature control to an accuracy of $\pm$ 1 °C was maintained during all the tensile tests.

After deformation the tensile specimens were quenched fast by a jet of liquid nitrogen and metallographic specimens were prepared from both the gauge and shoulder sections. These specimens were mechanically polished using 0.25 μm diamond paste at the final stage. The etching was done with a modified Keller's reagent containing HF:HCl:HNO_3:H_2O in proportions of 2:3:5:190. Grain sizes were measured with a Leitz Tas Plus image analyser by considering 1000 grains or more in each specimen. No distinction between the phases was made for the purpose of reporting grain sizes here. The error in grain size was within $\pm$ 5% at 95% confidence limit.

3. Results

3.1. Effect of strain rate

In order to study the effect of strain rate on grain growth, separate tensile specimens were deformed at the constant strain rates of 10^{-5}, 10^{-4}, 10^{-3} and $10^{-2}\,s^{-1}$. The test temperature was kept constant at 540 °C. At each strain rate, separate specimens were deformed to at least three selected strains for getting grain size data as a function of strain. Two strains of 0.30 and 0.70 were selected to be common for each strain rate.

0022–2461/91 $03.00 + .12

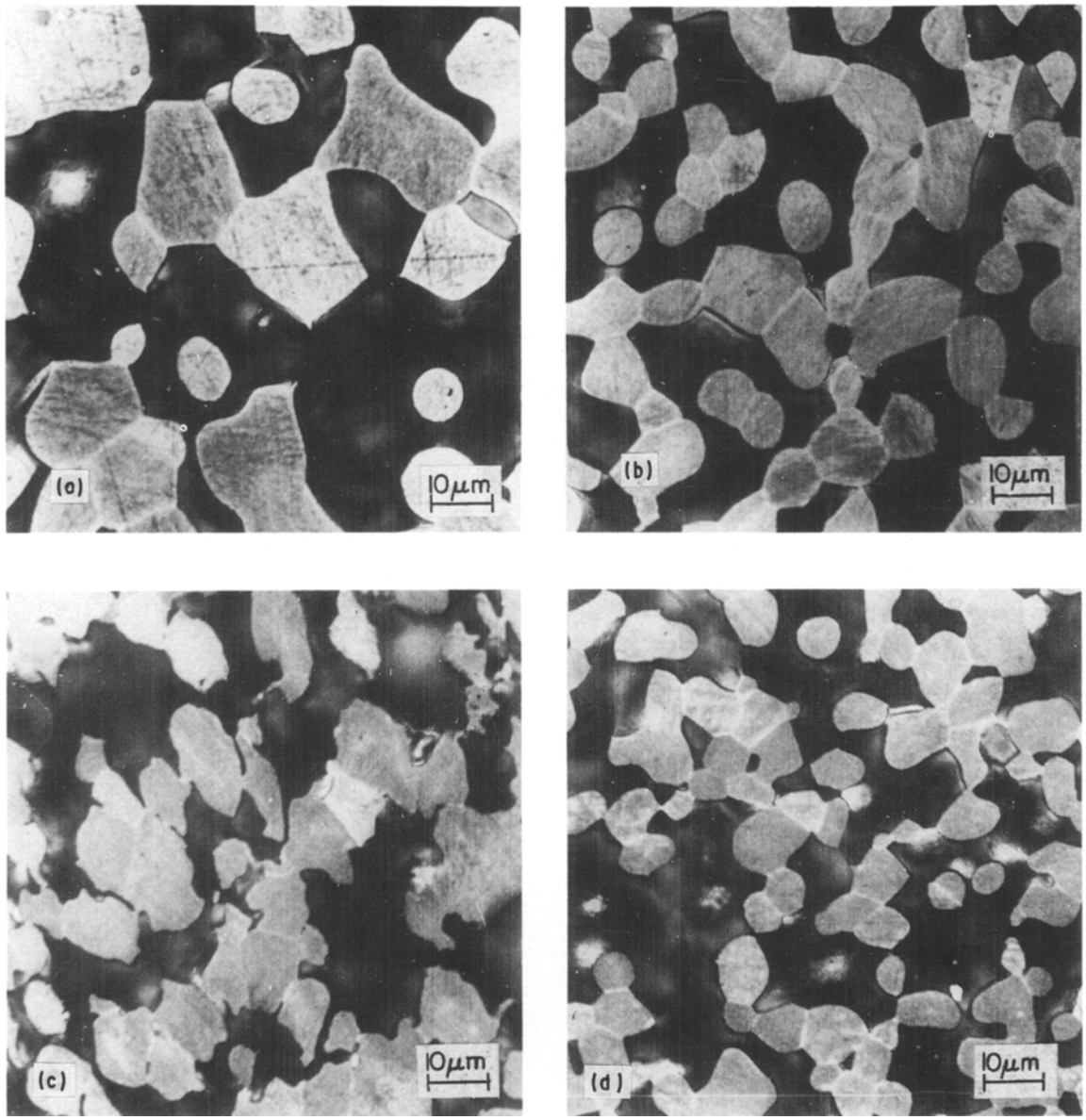

Figure 1 Micrographs illustrating enhanced grain growth on deformation ($\varepsilon \approx 1.4$) at $T = 540\,°C$. $\dot{\varepsilon} = 10^{-5}\,s^{-1}$: (a) gauge, (b) shoulder; and $\dot{\varepsilon} = 10^{-2}\,s^{-1}$: (c) gauge, (d) shoulder.

Fig. 1 shows microstructures of the gauge and shoulder sections of two tensile specimens deformed at the strain rates of 10^{-5} and $10^{-2}\,s^{-1}$. It is seen that the grain growth is more in the specimen deformed at the lower strain rate. Further, the grain sizes of the gauge sections are larger than those of the shoulder sections. The grain boundaries in the microstructure of the deformed gauge section at $\dot{\varepsilon} = 10^{-2}\,s^{-1}$ appear zig-zag. The grain size data from both the shoulder (d_s) and gauge (d_g) sections are plotted as a function of time in Fig. 2. To reach the same strain level, the time involved is inversely proportional to strain rate. Therefore the grain sizes corresponding to the lower strain rates lie towards the longer time scale, whereas those corresponding to the higher strain rates appear towards the short time range in the figure. Different symbols have been used in Fig. 2 to distinguish the grain sizes obtained from the gauge sections of the specimens deformed at different strain rates. It is seen that the grain size increases with time (strain) in both the shoulder and gauge sections. The grain sizes in the

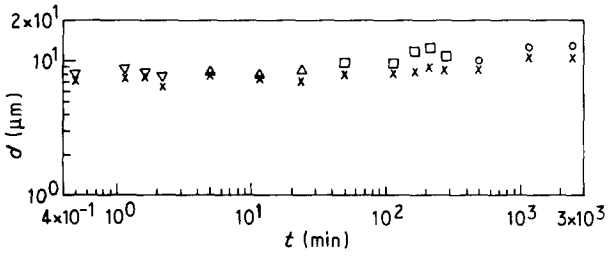

Figure 2 Grain size versus time plotted for the gauge and shoulder sections of tensile specimens deformed at different strain rates at 540 °C. Gauge: $\dot{\varepsilon}(s^{-1}) = (\bigcirc)\ 10^{-5}$, $(\square)\ 10^{-4}$, $(\triangle)\ 10^{-3}$, $(\triangledown)\ 10^{-2}$; shoulder: (×) all strain rates.

gauge sections are found to be larger than those in the corresponding shoulder sections. The extent of grain growth, for a fixed strain interval, decreases as the strain rate increases.

Grain growth in the gauge section ($d_{\varepsilon,t} = d_g - d_0$) occurs by both static annealing, i.e. time at high temperature (subscript t has been used to represent

this), as in the case of the shoulder section, and additionally by the imposed straining (subscript ε has been used to represent this). The strain size (d) during static annealing obeys the relation [16] $d \propto t^{0.1}$, t being the duration of annealing and 0.1 the value of the time exponent (n) in the grain growth kinetic law. Evaluation of the time exponent using grain sizes of the gauge sections (Fig. 2), suggested a slightly higher value, especially at lower strain rates.

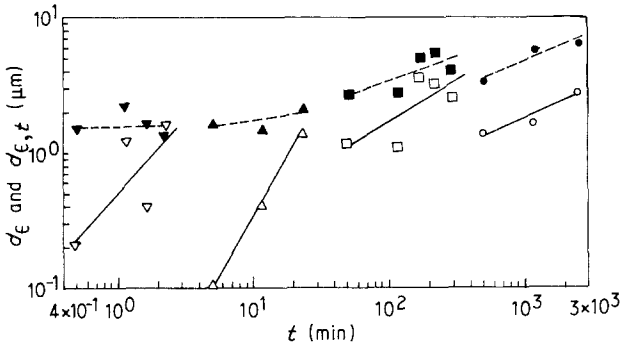

Figure 3 Contribution of straining, $d_\varepsilon = d_g - d_s$, to (—·—) overall grain size changes, $d_{\varepsilon,t} = d_g - d_0$, in the gauge section as a function of straining time at different strain rates. $T = 540\,^\circ$C. For d_ε, $\dot{\varepsilon}(s^{-1})$ = (○) 10^{-5}, (□) 10^{-4}, (△) 10^{-3}, (▽) 10^{-2}; for $d_{\varepsilon,t}$, $\dot{\varepsilon}(s^{-1})$ = (●) 10^{-5}, (■) 10^{-4}, (▲) 10^{-3}, (▼) 10^{-2}.

The difference in grain sizes between the gauge and shoulder sections is plotted (solid line, $d_\varepsilon = d_g - d_s$) as a function of time in Fig. 3. Also included in this figure is the plot of the change in grain size (broken line, $d_{\varepsilon,t} = d_g - d_0$) of the gauge section with respect to its initial grain size. The straight lines drawn are based on regression analysis. It is seen that $d_{\varepsilon,t}$ as well as d_ε increase with increasing time (strain) and decreasing strain rate. The proportion of grain growth due to straining alone varies between 40 and 60% at low strain rates (10^{-5} and $10^{-4}\,s^{-1}$) but at high strain rates there appear much wider variations in the contribution of straining. While the slope of $\log d_\varepsilon$ versus $\log t$ plots are generally seen to increase with increase in strain rate, the slope of $\log d_{\varepsilon,t}$ versus $\log t$ plots decreases with increasing strain rate. The rates of grain growth in both cases, namely $\Delta d_\varepsilon/\Delta t$ and $\Delta d_{\varepsilon,t}/\Delta t$ (not the ratio of logs) on the basis of the data in Fig. 3, however, increase with increase in strain rate, except for $\Delta d_{\varepsilon,t}/\Delta t$ at $\dot{\varepsilon} = 10^{-2}\,s^{-1}$. The rates of grain growth for the strain interval 0 to 30% are plotted as a function of strain rate in Fig. 4. Though the actual magnitude of the rate of grain growth will vary with the strain (time) interval considered, the grain growth resulting from simultaneous static annealing and deformation ($\Delta d_{\varepsilon,t}/\Delta t$) is more than that due to deformation ($\Delta d_\varepsilon/\Delta t$) alone (Fig. 4). The strain rate depend-

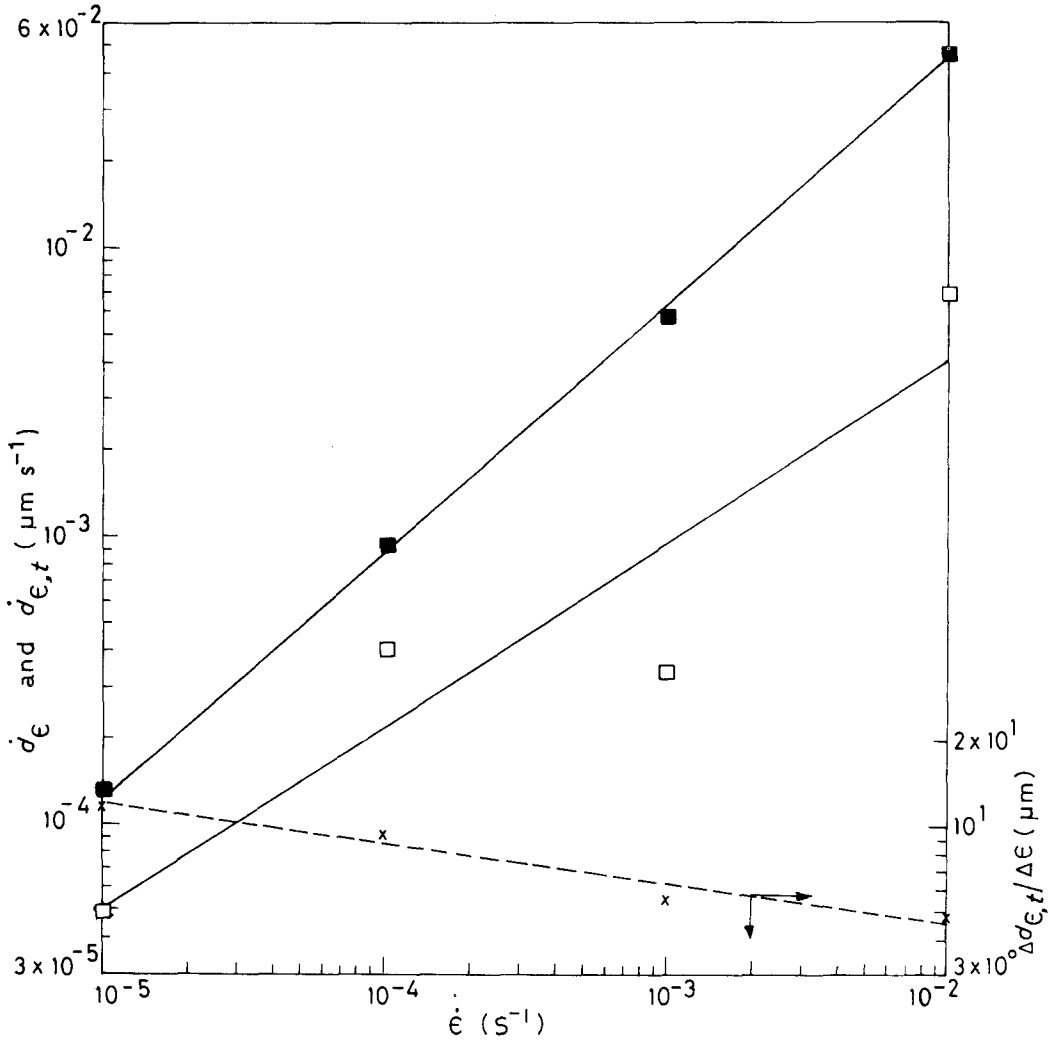

Figure 4 Plots of (■) grain growth rate ($\Delta d_{\varepsilon,t}/\Delta t$) due to combination of straining and time at high temperature versus strain rate; and (□) grain growth rate ($\Delta d_\varepsilon/\Delta t$) due to straining alone, versus strain rate. Also included is (×) plot of overall grain growth per unit strain ($\Delta d_{\varepsilon,t}/\Delta\varepsilon$) as a function of strain rate. $\Delta\varepsilon = 0.30$.

ences of the rate of grain growth in these two cases are determined to be $\dot{d}_{\varepsilon,t} \propto \dot{\varepsilon}^{0.86}$ and $\dot{d}_{\varepsilon} \propto \dot{\varepsilon}^{0.64}$.

The grain growth per unit strain, on the other hand, is seen to decrease with increase in strain rate because of the inverse relation between strain rate and time ($\Delta t = \Delta\varepsilon/\dot{\varepsilon}$). The dashed line in Fig. 4, for instance, is based on $\Delta d_{\varepsilon,t}/\Delta\varepsilon$ versus $\dot{\varepsilon}$ data for $\Delta\varepsilon = 0.30$. The relation between this plot and $\Delta d_{\varepsilon,t}/\Delta t$ versus $\dot{\varepsilon}$ can be realized through the fact that, unlike the constant magnitude of 0.30 for $\Delta\varepsilon$, Δt (for this strain interval) is an inverse function of the strain rate. Accordingly, $\Delta d_{\varepsilon,t}/\Delta\varepsilon = \Delta d_{\varepsilon,t}/(\dot{\varepsilon} \times \Delta t)$ and the difference between the two plots will be equal to the magnitude of the applied strain rate which itself constitutes the abscissa of the plots in Fig. 4.

3.2. Effect of temperature

Separate tensile specimens were deformed to strains of 0.30 and 0.70 at selected temperatures in the range 400 to 540 °C. The strain rate used was $10^{-4}\,s^{-1}$. The grain sizes measured from the shoulder and gauge sections after deformation are listed in Table I. The grain sizes in the gauge sections are again larger than that in the shoulder sections.

The change in grain size ($d_{\varepsilon,t}$) of the gauge section with respect to its initial value has been used to evaluate the activation energy ($Q_{\varepsilon,t}$) for grain growth. The Arrhenius plot is given for strains of 0.30 and 0.70 in Fig. 5. The activation energy for grain growth

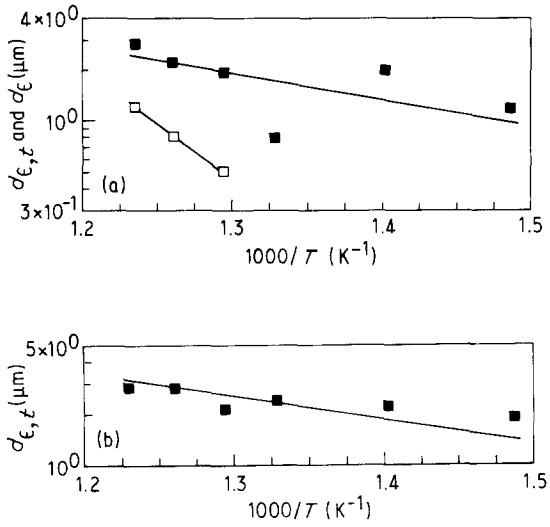

Figure 5 (■) Arrhenius plots to evaluate activation energy from $d_{\varepsilon,t}$ for grain growth during superplastic deformation: (a) $\varepsilon = 0.30$, (b) $\varepsilon = 0.70$. (□) Plot using change in grain size d_{ε} arising from straining alone at $\varepsilon = 0.30$ only. $\dot{\varepsilon} = 10^{-4}\,s^{-1}$.

was calculated assuming a relation $d_{\varepsilon,t} \propto \exp(-Q_{\varepsilon,t}/RT)$, where RT has its usual meaning. The activation energy for grain growth (using regression analysis) was found to be 84 and 74 kJ mol^{-1} at $\varepsilon = 0.30$ and 0.70, respectively, which give an average $Q_{\varepsilon,t} = 79$ kJ mol^{-1}.

An attempt was also made to estimate the activation energy for grain growth due to deformation alone (Q_{ε}) assuming a relation $d_{\varepsilon} \propto \exp(-Q_{\varepsilon}/RT)$. There appeared to be very large scatter in d_{ε}, especially at lower temperatures (400–480 °C) and at the larger strain ($\varepsilon = 0.70$). The scatter in d_{ε} was so much that the activation energy was evaluated (d_{ε} at various temperatures can be obtained from the data in Table I) satisfactorily only at $\varepsilon = 0.30$ over the temperature range of 500 to 540 °C, giving $Q_{\varepsilon} = 200$ kJ mol^{-1}. The corresponding Arrhenius plot is included in Fig. 5a.

4. Discussion

The Al–Cu eutectic alloy under tensile tests at the elevated temperatures and low strain rates required for superplasticity exhibits grain growth. The rate of grain growth increases with strain rate according to $\dot{d}_{\varepsilon,t} \propto \dot{\varepsilon}^{0.86}$. A similar relationship was also shown during superplastic deformation of an Ni–Cr–Fe alloy [1]. Both static annealing and concurrent straining contribute to the observed grain growth in the gauge section. The relative contributions of these components depend on the strain rate and temperature as discussed below.

For static grain growth [16] of the type $d \propto t^{0.1}$, the grain size of the shoulder section (d_s) of the specimen deformed at $\dot{\varepsilon} = 10^{-5}\,s^{-1}$ is expected to be twice the size at $\dot{\varepsilon} = 10^{-2}\,s^{-1}$, based on the times needed for deforming the specimens to the same strain. However, on the same (grain size and time) basis, the rate of grain growth ($\Delta d_s/\Delta t$) at $\dot{\varepsilon} = 10^{-2}\,s^{-1}$ should be 500 times higher than that at the lower strain rate since $t = \varepsilon/\dot{\varepsilon}$. A similar argument is applicable to the grain growth associated with straining because of the small difference in grain sizes for the large difference in the strain rates.

In Sn–1% Bi alloy, Clark and Alden [3] have found that the plots of strain rate sensitivity ($m = \partial(\log\sigma)/\partial(\log\dot{\varepsilon})$) versus $\log\dot{\varepsilon}$ and normalized grain growth per unit strain versus $\log\dot{\varepsilon}$ are similar. Recently the grain size in a microduplex stainless steel has also been suggested to increase with m [6]. Senkov and Myshlyaev [8] have pointed out that the similarity between the two plots in Sn–1% Bi alloy [3] has no physical meaning but by chance it results from the

TABLE I Grain sizes of gauge (d_g) and (d_s) sections upon tensile tests ($\dot{\varepsilon} = 10^{-4}\,s^{-1}$) at different temperatures ($d_0 = 6.5$ μm)

ε	Section	Grain size (μm)					
		540 °C	520 °C	500 °C	480 °C	440 °C	400 °C
0.30	Gauge	9.3	8.7	8.4	7.3	8.5	7.7
	Shoulder	8.1	7.9	7.9	7.5	7.5	6.8
0.70	Gauge	9.3	9.3	8.6	8.9	8.7	8.4
	Shoulder	8.2	7.9	8.3	7.0	7.1	7.3

method that was adopted in the treatment of the data. In the Al–Cu eutectic alloy the slopes (n_ε) of $\log d_\varepsilon$ versus $\log t$ (Fig. 3) at low strain rates seem to be comparable with the value of m reported earlier [13], but at higher strain rates n_ε values are much larger than m. However, it is felt that since with increasing strain rate the flow stress increases and the dependence is well represented by m, some suitable parameter of the deformation enhanced grain growth (d_ε) should also correlate with m. It is interesting that the slope of the $\log \dot{d}_\varepsilon$ versus $\log \dot{\varepsilon}$ line ($g = 0.64$) in Fig. 4 seems comparable with m (0.67).

The temperature dependence of grain growth is two-fold. First, as in static annealing, higher grain growth is expected as the temperature increases. Secondly, the stress required for deformation decreases with increasing temperature, which is expected to have a similar consequence for d_ε as has the decrease in strain rate. While the activation energies for grain growth in these two cases may be associated with two separate thermally activated processes, it becomes difficult to understand the meaning of $Q_{\varepsilon,t}$ when grain growth results from both the effects together. Then the activation energy probably represents how these two effects align themselves for grain growth, namely whether they operate in series or parallel.

The Al–Cu eutectic alloy contains Al-rich ($\mathscr{H}$) and $CuAl_2$ (θ) phases. Grain growth in this system should involve diffusion of atoms of Al and/or Cu through these phases and across the boundaries of types Al–Al, Al–θ or θ–θ. If the atom movement is sequential then the activation energy for grain growth should be comparable with the highest activation energy value for lattice diffusion (Q_1) in the participating phase(s). The values of Q_1 for Al and θ phases are 142 kJ mol^{-1} [17] and 123 kJ mol^{-1} [18], respectively. If the atoms move independently along the boundaries and in the grains then the activation energy for grain growth should be in the range of activation energies for grain boundary diffusion (Q_{gb}) or interphase boundary diffusion. Taking $Q_{gb} = 0.6\ Q_1$ [19], the activation energy for grain boundary diffusion along Al–Al and θ–θ phases becomes 85 and 74 kJ mol^{-1}, respectively. The activation energy for diffusion along the interphase boundary has been reported [20] to be 98 kJ mol^{-1}. The observed activation energy for the grain growth (79 kJ mol^{-1}) falls in this range of values. It is therefore suggested that grain growth under the combination of static annealing and deformation occurs by grain boundary diffusion. From the grain boundary migration experiments in a zone-refined aluminium the activation energy for migration has been reported to be in the range of 55 to 67 kJ mol^{-1} [21, 22].

The value of activation energy (200 kJ mol^{-1}) for grain growth (d_ε) over 500 to 540 °C purely on the basis of deformation seems to be more toward the activation energy for deformation itself [12]. It may be possible that the mechanisms of grain growth and deformation have some common step that becomes rate-controlling. In view of the sequential nature of the grain boundary sliding and migration [6], the activation energy for deformation may correspond to that of the grain boundary migration which occurs as the accommodation process for grain boundary sliding. Grain boundary migration involves diffusion of atoms from one lattice to another and across the boundary, in which case it should be feasible that the activation energy for grain growth due to deformation may correspond to the activation energy for lattice diffusion (Q_1 for Cu = 211 kJ mol^{-1} [23]).

The increase in grain size results in the requirement of a higher stress for deformation at elevated temperature. However, at larger strains and relatively lower temperatures there occurs significant cavitation in the Al–Cu eutectic alloy [15]. The presence of cavities reduces the stress required for deformation [13]. The oppposite dependences of stress on grain size and cavity level make the analysis of the temperature effect on grain growth complex. Thus, the absence of a systematic effect of temperature on grain growth below 500 °C as well as at 70% strain (as was evident from the large scatter in d_g) may be due to the dominance of cavitation.

Grain growth due to straining is related to the strain rate and temperature by g and Q_ε, respectively, in the same way as the stress for superplastic deformation is related to the strain rate and temperature by m and Q. Therefore, the stress may be a more appropriate parameter to be considered in the way it affects the phenomena responsible for grain growth. Logσ versus log$\dot{\varepsilon}$ plots during high-temperature deformation of several superplastic materials exhibit three distinct regions. Superplastic behaviour ($m \geqslant 0.3$) is seen at intermediate strain rates. Now it is known that grain boundary sliding dominates in this region. At lower strain rates grain boundary sliding is accommodated by diffusion, whereas at higher strain rates the accommodation is provided by intragranular slip [24]. Both these accommodation processes are also related to grain boundary migration, which is seen to accompany grain boundary sliding in order to relieve the stress concentration built up by sliding [25]. Grain rotation is another phenomenon observed during superplastic deformation. At any strain rate all these processes occur but to varying extents. Grain boundary sliding is thought [25] to occur by glide and climb of extrinsic grain boundary dislocations. The formation of extrinsic grain boundary dislocations and their participation in sliding may increase the vacancy concentration in the vicinity of the grain boundary. In Zn–0.4% Al alloy the vacancy concentration has been shown to increase with strain rate [26]. In the superplastic region it is, therefore, suggested that the grain boundary sliding rate increases with increasing stress [25] which, in turn, provides a higher vacancy concentration for the enhanced grain boundary migration through diffusion.

It may be worth noting that the microstructure obtained on straining at a low strain rate (10^{-5} s^{-1}) does not show any change in grain morphology. This microstructure resembles very well that obtained on prolonged static annealing [16]. Thus, grain growth at the low strain rate may be more by the mechanism which prevails during static annealing. The stress seems to enhance the grain growth through rapid diffusion along the migrating boundary [27, 28]. In

contrast, the microstructure on straining at a high strain rate ($10^{-2}\,s^{-1}$) reveals zig-zag boundaries [13]. The zig-zag boundaries have been suggested to be formed by the emission and accumulation of edge dislocations from the region of stress concentration in the grain boundaries, their polygonization and finally grain boundary migration toward the polygonized groups to equalize interfacial tension [29]. The presence of such boundaries may help grain growth in two ways. Firstly, the ridges in the boundary may act as a barrier against further sliding, but due to the higher stress for deformation the sliding rate should be high [25] in the local planar boundaries. The higher sliding rate builds up stress concentration faster at the barrier and thus creates a situation for the enhanced grain boundary migration rate. Secondly, the zig-zag boundaries, through an increased grain boundary area, increase the driving force for grain boundary migration. Thus, partly due to this reason also the rate of grain growth at $\dot{\varepsilon} = 10^{-2}\,s^{-1}$ should become higher than that at $\dot{\varepsilon} = 10^{-5}\,s^{-1}$.

5. Conclusions

1. Both static annealing and deformation at high temperature contribute almost equally to the observed grain growth at low strain rates. At high strain rates the proportion of deformation-associated grain growth varies widely, depending on the strain.

2. The rate of grain growth increases with strain rate mainly because the difference in the times required for reaching a fixed strain at any two strain rates is much larger as compared to the corresponding difference in the grain sizes.

3. The activation energy for grain growth is found to be $79\,kJ\,mol^{-1}$, which suggests that the grain growth occurs by grain boundary diffusion under the condition of annealing and concurrent straining.

4. Strain rate and temperature influence the strain-induced grain growth in the same way as they do the stress required for superplastic deformation.

References

1. R. J. LINDINGER, R. C. GIBSON and J. H. BROPHY, *Trans. ASM* **62** (1969) 230.
2. B. M. WATTS and M. J. STOWELL, *J. Mater. Sci.* **6** (1971) 228.
3. M. A. CLARK and T. H. ALDEN, *Acta Metall.* **21** (1973) 1195.
4. G. RAI and N. J. GRANT, *Metall. Trans.* **6A** (1975) 385.
5. M. SUÈRY and B. BAUDELET, *Rev. Phys. Appl.* **13** (1978) 53.
6. B. P. KASHYAP and A. K. MUKHERJEE, *J. Mater. Sci.* **18** (1983) 3299.
7. D. S. WILKINSON and C. H. CACERES, *Acta Metall.* **32** (1984) 1335.
8. O. N. SENKOV and M. M. MYSHLYAEV, *ibid.* **34** (1986) 97.
9. D. L. HOLT and W. A. BACKOFEN, *Trans. ASM.* **59** (1966) 755.
10. M. J. STOWELL, J. L. ROBERTSON and B. M. WATTS, *Metal Sci. J.* **3** (1969) 41.
11. K. A. PADMANABHAN and G. J. DAVIES, *Metal Sci.* **11** (1977) 177.
12. B. P. KASHYAP and K. TANGRI, *Scripta Metall.* **19** (1985) 1419.
13. *Idem., Metall. Trans.* **18A** (1987) 417.
14. A. H. CHOKSHI and T. G. LANGDON, *ibid.* **19A** (1988) 2487.
15. B. P. KASHYAP and K. TANGRI, *ibid.* **20A** (1989) 453.
16. *Idem., Z. Metallk.* **78** (1987) 876.
17. T. S. LUNDY and J. S. MURDOCH, *J. Appl. Phys.* **33** (1962) 1671.
18. Y. FUNAMIZU and K. WATANABE, *Trans. JIM* **12** (1971) 147.
19. H. J. FROST and M. F. ASHBY, "Deformation Mechanism Maps" (Pergamon, Oxford, 1982) p. 21.
20. E. HO and G. S. WEATHERLY, *Acta Metall.* **23** (1975) 1451.
21. K. T. AUST, "New Physical and Chemical Properties of Very High-Purity Metals" (Centre National de la Recherche Scientifique, Paris, 1960) p. 99.
22. P. GORDON and R. A. VANDERMEER, *Trans. AIME* **224** (1962) 917.
23. S. J. ROTHMAN and N. L. PETERSON, *Phys. Status Solidi* **35** (1969) 305.
24. M. F. ASHBY and R. A. VERRALL, *Acta Metall.* **21** (1973) 149.
25. H. GLEITER and B. CHALMERS, *Prog. Mater. Sci.* **16** (1972) 179.
26. O. A. KAIBYSHEV, I. V. KAZACHKOV, V. V. ASTANIN and B. V. RODIONOV, *Izv. vuzov. Tsvetnaya Metallurgia* **3** (1974) 127.
27. M. HILLERT and G. R. PURDY, *Acta Metall.* **26** (1978) 333.
28. K. SMIDODA, W. GOTTSCHALK and H. GLEITER, *Acta Metall.* **26** (1978) 1833.
29. J. L. LYTTON, C. R. BARRETT and O. D. SHERBY, *Trans. AIME* **223** (1965) 1399.

Received 30 April
and accepted 20 December 1990